Supporting Information for

Fullerene-Free Polymer Solar Cells Enabled with A PhI-Based Wide Bandgap Donor Polymer: Promoting Efficiencies via Acceptor Screening and Device Engineering

Huifeng Meng,[a,b] Yongchun Li,[a,b] Bo Pang,[a] Yuqing Li,[a,b] Chuanlang Zhan,[b] Jianhua Huang,*[a]*

[a] College of Materials Science and Engineering, Huaqiao University, Xiamen, 361021, P. R. China.

[b] CAS key Laboratory of Photochemistry, Institute of Chemistry, Chinese Academy of Sciences, Beijing 100190 China

Contents

1 Experimental Section

1.1 Materials and Instruments

PBDT-PhI was synthesized according to our previous work.[1] The number-averaged molecular weight (M_n), weight-averaged molecular weight (M_w), and polydispersity index (PDI) of PBDT-PhI were 2.93×10^4 Da, 4.27×10^4 Da, and 1.46, respectively, tested by gel permeation chromatography (GPC, Waters). All reagents were purchased from Sigma-Aldrich, Acros, Alfa Aesar or TCI and used as received. Non-fullerene acceptors (ITIC, IT-4F, ITCT, and IEICO-4F), PDINO, and PEDOT: PSS (Baytron Clevios P VP AI 4083, Germany) were purchased from Solarmer company. Absorption spectra were recorded on a Hitachi U-3010 UV−vis spectrophotometer and carried out at room temperature. The thickness of the solid films was measured using a Dektak Profilometer. Cyclic voltammetry was performed under an inert atmosphere at a scan rate of 0.1 V s^{-1} with 0.1 M tetrabutylammonium hexafluorophosphate in acetonitrile as the electrolyte and used a glassy-carbon, a platinum-wire, and an Ag/AgCl, respectively, as work, auxiliary, and reference electrodes. The EQE data were obtained using a solar cell spectral response measurement system (QE-R3011, Enli Technology Co. Ltd). Atom Force Microscopy (AFM) images were obtained by Brucker Multimode 8 using scanmode. TEM tests were performed on a JEM-2011F operated at 200 kV. TEM samples were obtained by transferring the floated blend films from the water onto the Cu grid. All the blend films were fabricated under the optimal conditions. The XRD pattern was recorded by a Rigaku D/max–2500 diffractometer operated at 40 kV voltage and a 200 mA current with Cu Kα radiation. The XRD samples were prepared by spin-coating on silica substrates in with the same conditions to the device preparation. The ultraviolet photoelectron spectroscopy (UPS) samples were prepared by spin-coating the solutions on quartz substrates. Samples were analyzed on Thermo Scientific ESCALab 250Xi using UPS, The gas discharge lamp was used for UPS, with helium gas admitted and the HeI (21. 22eV) emission line employed. The helium pressure in the analysis chamber during a nalysis was about 3E-8 mbar. The data were acquired with –10 V bias. The HOMO energy levels were calculated from $E_{HOMO} = E_{cutoff} - E_{onset} - h\nu$, where E_{cutoff} and E_{onset} are obtained from the UPS spectra, hν is 21.22 eV.

1.2 Gaussian Calculations

Density functional theory (DFT) calculations were performed using the Gaussian 09 program with the B3LYP exchange-correlation functional.[2-4] All-electron triple- ξ valence basis sets with polarization functions (6-31G (d, p)) are used for all atoms. Geometry optimizations were performed with full relaxation of all atoms. All alkyl chains were reduced to methyl groups for avoiding computational load. For each molecule, various conformations with different dihedral angles were optimized, and the data for the one with the lowest energy are reported.

1.3 Fabrication and Tests of Photovoltaic devices

Photovoltaic devices with a conventional configuration of ITO/PEDOT: PSS/Active Layer/ETL/Al was fabricated as follows: The ITO glasses were pre-cleaned with sequential ultrasonication in a soap-deionized water mixture deionized water, CMOS grade acetone and isopropanol in turn for 15 min, respectively. The washed substrates were further treated with oxygen plasma for 30 min to eliminate any remaining organic components. Then a thin layer (approximately 20 nm) of PEDOT: PSS (poly(3,4-ethylenedioxythiophene)-poly(styrenesulfonate)) was spin-coated at 6000 RPM for 30 s and baked in oven at 150 °C for 20 min. The photovoltaic layer (PBDT-PhI: acceptor) with the optimized D/A ratio were spin-coated at 1500 rpm for 50 s and then thermally annealed at 100 °C for 10 min. Processing additive DIO was optimized to 1%(v/v). The concentration of each solution was kept to be 20 mg/ml. Atop of active layer a methanol solution of ETL PDINO (optimized concentration 1 mg/ml) was spin-coated with rotation speed of 3000 rpm for 30 s. Finally Al (ca. 80 nm) was thermally deposited under the vacuum of 1×10^{-6} Torr. The active area of the device was 0.04 cm^2. The devices were characterized in nitrogen atmosphere under the illumination of simulated AM 1.5G (AAA grade, XES-70S1) light source. The illumination intensity in front of the cell sample was calibrated to be 100 mW/cm^2 with a reference silicon cell. The current density-voltage (*J-V*) measurement of the devices was recorded along the forward scan direction from -1.5 to 1.5 V using a computer-controlled Keithley 2400 Source Measure Unit.

1.4 Measurements of Electron and Hole Mobilities by the Space-Charge Limited Current (SCLC) Method

The electron-only devices were fabricated with a configuration of ITO/titanium (diisopropoxide) bis(2,4-pentanedionate) (TIPD)/active layer/PDINO/Al and hole-only devices were configured with ITO/PEDOT:PSS/active layer/ Au. The TIPD buffer layer was prepared by spin-coating a 3.5 wt % TIPD isopropanol solution onto the pre-cleaned ITO substrate and then baked at 150 °C for 10 min to convert TIPD into TOPD.[5] Subsequently, the blend was spin-coated on it under the same condition as preparation of the optimal solar cells. The Al layer was thermally deposited on the top of the blend in vacuum at a speed of 1 Å/ s. The electron and hole mobilities were extracted by fitting the current density-voltage curves using the Mott-Gurney law,[6,7]

$$J_{SCL} = \frac{9\varepsilon\varepsilon_0\mu V^2}{8L^3}$$

where ε is the dielectric constant of the organic component, ε_0 is the permittivity of the vacuum (8.85419×10^{-12} $CV^{-1}m^{-1}$), μ is the zero-field mobility, J_{SCL} is the current density, L is the thickness of the active layer, and $V = V_{app} - V_{bi}$, here V_{app} is the applied potential, and V_{bi} the built-in potential which results from the difference in the work function values of the cathode. From the plot of $J^{1/2}$ versus V, the hole and

electron mobilities can be deduced.

2 Supporting Figures and Tables

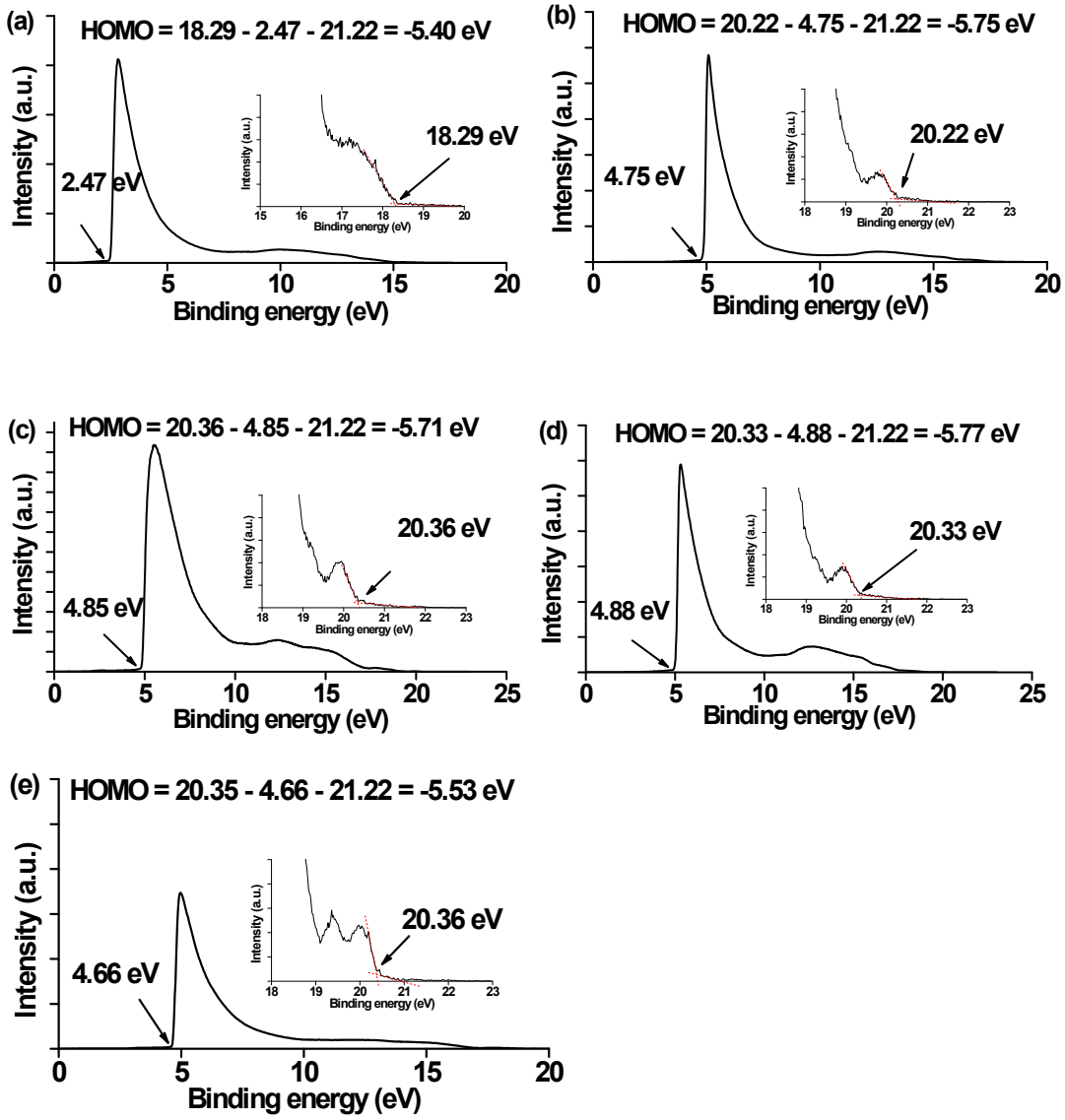

Figure S1. UPS spectra and corresponding HOMOs of PBDT-PhI (a), IT-4F (b), ITIC (c), ITCT (d), and IEICO-4F (e).

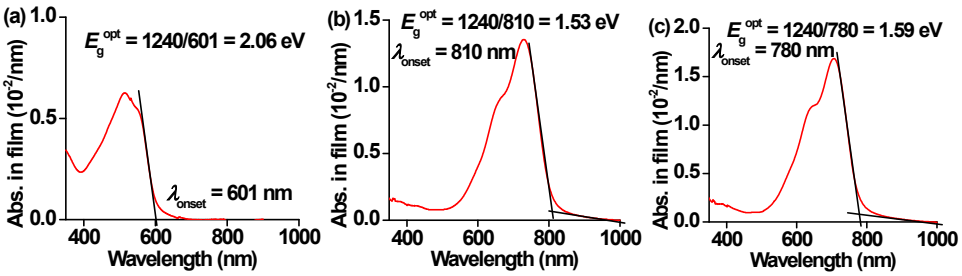

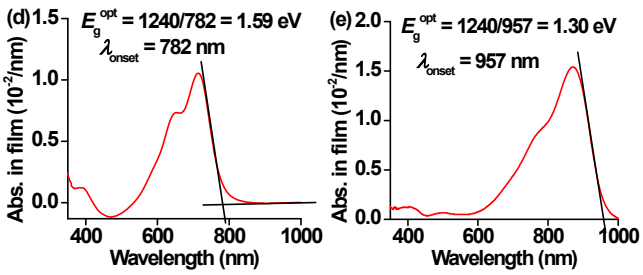

Figure S2. Film absorption spectra and calculations of optical bandgaps of PBDT-PhI (a), IT-4F (b), ITIC (c), ITCT (d), and IEICO-4F (e).

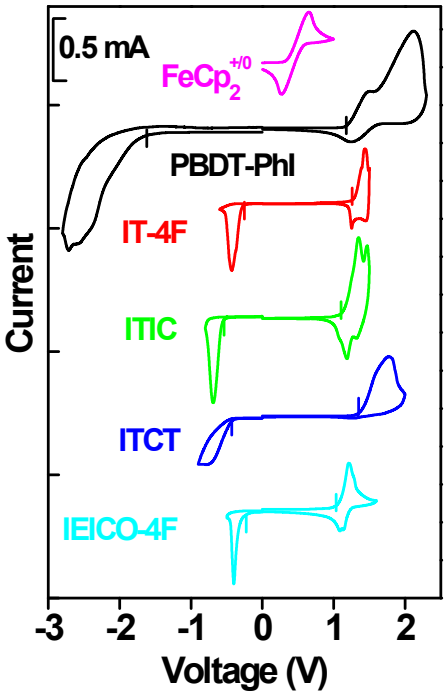

Figure S3. CV curves of PBDT-PhI, IT-4F, ITIC, ITCT, and IEICO-4F. $FeCp_2$ was utilized as the internal standard.

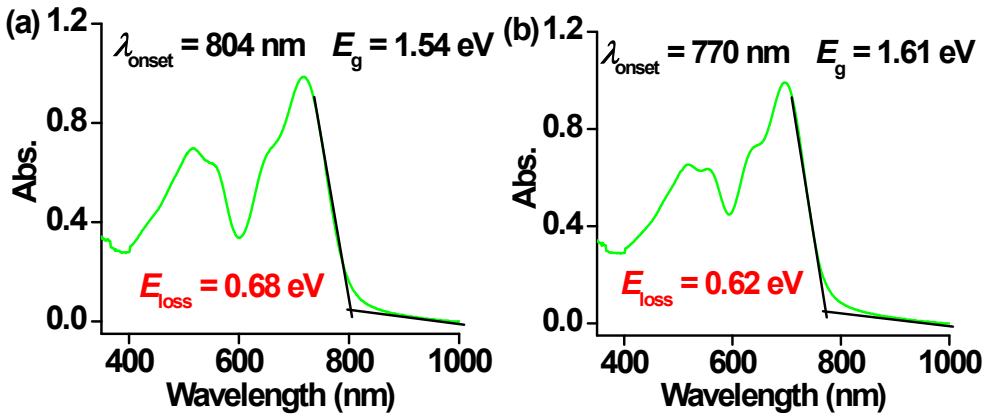

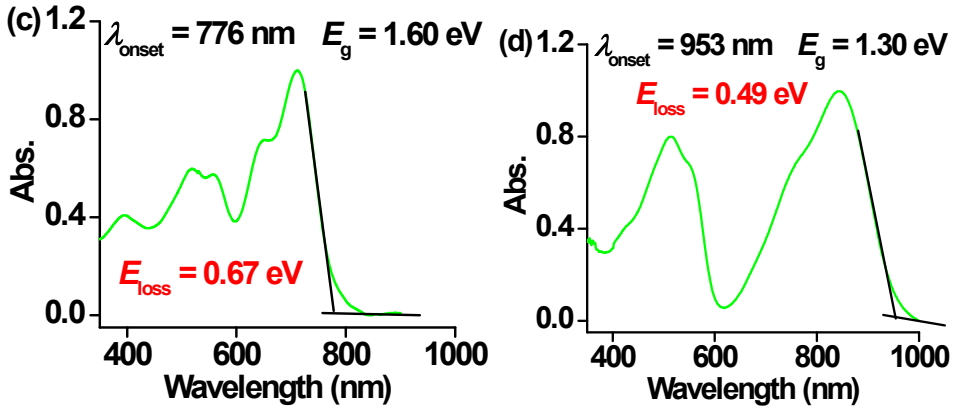

Figure S4. Absorption spectra of blending films and calculations of V_{loss} of the four devices.

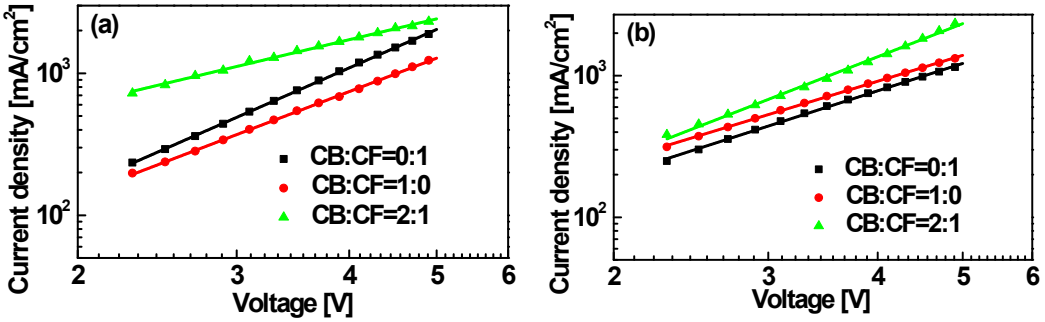

Figure S5. *J-V* plots tested by SCLC methods for hole (a) and electron (b)-only devices.

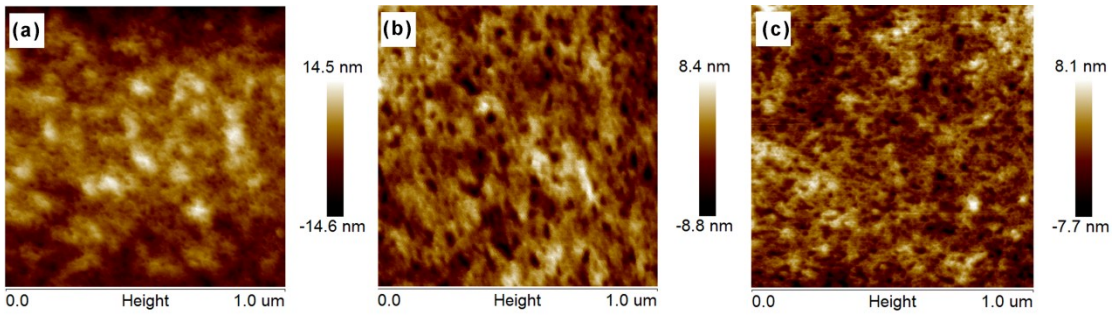

Figure S6. AFM height images of active layers spin-coated from CF (a, R_a = 3.37 nm), CB (b, R_a = 1.90 nm), and CB/CF (c, R_a = 1.74 nm).

Table S1. HOMO and LUMO energy levels estimated from different tests.

	Estimated from CV				Estimated from UPS and E_g^{opt}		
Compounds	E_{onset}^{ox} **(V)**	E_{onset}^{red} **(V)**	**HOMO (eV)**	**LUMO (eV)**	E_g^{opt} **(eV)**	**HOMO (eV)**	**LUMO (eV)**
PBDT-PhI	1.16	-1.60	-5.50	-2.74	2.06	-5.40	-3.34
IT-4F	1.26	-0.26	-5.60	-4.08	1.53	-5.75	-4.22
ITIC	1.10	-0.54	-5.44	-3.80	1.59	-5.71	-4.12
ITCT	1.33	-0.39	-5.67	-3.95	1.59	-5.77	-4.18

IEICO-4F	1.05	-0.22	-5.39	-4.12	1.30	-5.53	-4.23

Table 2. Device performances of PBDT-PhI/IT-4F with different contents of DIO and CN.

CN[v/v%)	**DIO[v/v%]**	V_{oc}**[V]**	J_{sc}**[mA/cm^2]**	**FF[%]**	**PCE[%]**
-	0	0.84	19.90	47.90	7.19 (6.93)[a]
-	0.5	0.84	17.92	50.87	7.68 (7.55)[a]
-	1	0.86	15.99	59.69	8.18 (7.89)[a]
-	1.5	0.82	17.19	56.28	7.95 (7.67)[a]
0.5	-	0.78	18.70	52.48	7.68 (7.46)[a]
1	-	0.78	19.04	53.46	7.94 (7.59)[a]
1.5	-	0.79	13.82	57.90	6.33 (6.10)[a]

[a] Statistic efficiencies averaged from 10 cells.

Table S3. Device performances of PBDT-PhI/ITIC with different DIO contents.

DIO[v/v%]	V_{oc}**[V]**	J_{sc}**[mA/cm^2]**	**FF[%]**	**PCE[%]**
0	0.99	19.90	47.90	7.57 (7.21)[a]
0.5	0.99	13.79	58.70	7.99 (7.68)[a]
1	0.99	12.00	52.65	6.27 (5.96)[a]
1.5	0.99	7.61	50.83	3.86 (3.75)[a]

[a] Statistic efficiencies averaged from 10 cells.

Table S4. Device performances of PBDT-PhI/IEICO-4F with different DIO contents.

DIO[v/v%]	V_{oc}**[V]**	J_{sc}**[mA/cm^2]**	**FF[%]**	**PCE[%]**
0	0.81	8.20	54.00	3.59 (3.12)[a]
1	0.81	9.26	51.95	3.90 (3.76)[a]

[a] Statistic efficiencies averaged from 10 cells.

Table S5. Device performances of PBDT-PhI/ITCT with different DIO contents.

DIO[v/v%]	V_{oc}**[V]**	J_{sc}**[mA/cm^2]**	**FF[%]**	**PCE[%]**
0	0.93	11.49	58.89	6.28 (6.02)[a]
0.5	0.93	12.79	63.72	7.57 (7.23)[a]
1	0.93	14.39	66.23	8.86 (8.70)[a]

1.5	0.93	10.56	63.28	6.21 (6.01)[a]

[a] Statistic efficiencies averaged from 10 cells.

Table S6. Device performances of PBDT-PhI/IT-4F with different solvents

Solvents	V_{oc}**[V]**	J_{sc}**[mA/cm²]**	**FF[%]**	**PCE[%]**
CF	0.86	15.99	59.69	8.18 (7.89)[a]
CB	0.80	11.69	65.32	6.10 (5.88)[a]
DCB	0.80	11.02	65.09	5.70 (5.52)[a]

[a] Statistic efficiencies averaged from 10 cells.

Table S7. Device performances of PBDT-PhI/ITIC with CB as spin-coating solvents and various DIO contents.

DIO[v/v%]	V_{oc}**[V]**	J_{sc}**[mA/cm²]**	**FF[%]**	**PCE[%]**
0	0.95	12.13	59.65	6.87 (6.55)[a]
0.5	0.95	12.85	58.61	7.17 (6.93)[a]
1	0.95	12.26	55.22	6.41 (6.18)[a]
1.5	0.99	10.22	57.05	5.81 (5.66)[a]

[a] Statistic efficiencies averaged from 10 cells.

Table S8. Device performances of PBDT-PhI/ITCT with CB as spin-coating solvents and various DIO contents.

DIO[v/v%]	V_{oc}**[V]**	J_{sc}**[mA/cm²]**	**FF[%]**	**PCE[%]**
0	0.93	13.68	60.71	7.50 (7.31)[a]
0.5	0.90	12.82	59.90	6.89 (6.52)[a]
1	0.92	15.00	66.39	9.17 (9.02)[a]
1.5	0.92	12.26	62.45	7.02 (6.88)[a]

[a] Statistic efficiencies averaged from 10 cells.

Table S9. Device performances of PBDT-PhI/ITCT prepared from CB/CF mix solvent with different ratios.

CB/CF[v:v]	V_{oc}**[V]**	J_{sc}**[mA/cm²]**	**FF[%]**	**PCE[%]**
0:1	0.94	14.07	57.22	7.57 (7.25)[a]
1:1	0.91	8.09	53.00	8.09 (7.88)[a]
2:1	0.92	16.42	57.15	8.59 (8.23)[a]

3:1	0.91	16.67	56.00	8.51 (8.20)[a]
1:0	0.92	13.95	60.10	7.71 (7.55)[a]

[a] Statistic efficiencies averaged from 10 cells.

Table S10. Device performances of PBDT-PhI/ITCT prepared from CB/CF (2:1) with different DIO contents.

DIO[v/v%]	**V_{oc}[V]**	**J_{sc}[mA/cm^2]**	**FF[%]**	**PCE[%]**
0	0.92	16.42	57.15	8.59 (8.32)[a]
0.5	0.91	17.36	55.06	8.70 (8.48)[a]
0.75	0.91	18.34	56.03	9.35 (9.10)[a]
1	0.92	16.67	66.30	10.17 (9.96)[a]
1.25	0.90	15.02	57.86	7.83 (7.63)[a]

[a] Statistic efficiencies averaged from 10 cells.

Table S11. XRD parameters of PBDT-PhI, ITCT, and the blend films spin-coated from different solvents.

Compounds	100		010	
	2θ(º)	d(Å)	2θ(º)	d(Å)
PBDT-PhI	4.36	20.27	24.58	3.62
ITCT	4.91	18.00	26.12	3.41
Blend-CF	4.85	18.22	25.07	3.55
Blend-CB	3.93	22.48	26.31	3.39
Blend-CB:CF	4.42	20.00	26.19	3.40

3 References

[1] Huang, J. H.; Wang, X., Zhan, C. L., Zhao, Y., Sun, Y. X., Pei, Q. B., Liu, Y. Q., Yao, J. N. Wide band gap copolymers based on phthalimide: synthesis, characterization, and photovoltaic properties with 3.70% efficiency. *Polym. Chem*. **2013**, *4*, 2174.

[2] M. J. Frisch, G. W. T., H. B. Schlegel, G. E. Scuseria, M. A. Robb, J. R. Cheeseman, J. A. Montgomery Jr., T. Vreven, K. N. Kudin, J. C. Burant, J. M. Millam, S. S. Iyengar, J. Tomasi, V. Barone, B. Mennucci, M. Cossi, G. Scalmani, N. Rega, G. A. Petersson, H. Nakatsuji, M. Hada, M. Ehara, K. Toyota, R. Fukuda, J. Hasegawa, M. Ishida, T. Nakajima, Y. Honda, O. Kitao, H. Nakai, M. Klene, X. Li, J. E. Knox, H. P. Hratchian, J. B. Cross, V. Bakken, C. Adamo, J. Jaramillo, R. Gomperts, R. E. Stratmann, O. Yazyev, A. J. Austin, R. Cammi, C. Pomelli, J. W. Ochterski, P. Y. Ayala, K. Morokuma, G. A. Voth, P. Salvador, J. J. Dannenberg, V. G. Zakrzewski, S. Dapprich, A. D. Daniels, M. C. Strain, O. Farkas, D. K. Malick, A. D. Rabuck, K. Raghavachari, J. B. Foresman, J. V.

Ortiz, Q. Cui, A. G. Baboul, S. Clifford, J. Cioslowski, B. B. Stefanov, G. Liu, A. Liashenko, P. Piskorz, I. Komaromi, R. L. Martin, D. J. Fox, T. Keith, M. A. Al-Laham, C. Y. Peng, A. Nanayakkara, M. Challacombe, P. M. W. Gill, B. Johnson, W. Chen, M. W. Wong, C. Gonzalez, and J. A. Pople, (Gaussian 03, Revision C.02, Gaussian, Inc., Wallingford CT, 2004).

[3] Becke, A. D., Density-functional exchange-energy approximation with correct asymptotic behavior. *Phys. Rev. A* **1988**, *38*, 3098.

[4] Lee, C.; Yang, W.; Parr, R. G., Development of the Colle-Salvetti correlation-energy formula into a functional of the electron density. *Phys. Rev. B* **1988**, *37*, 785.

[5] Tan, Z. A.; Zhang, W.; Zhang, Z.; Qian, D.; Huang, Y.; Hou, J.; Li, Y. High-performance inverted polymer solar cells with solution-processed titanium chelate as electron-collecting layer on ITO electrode. *Adv. Mater.*, **2012**, *24*, 1476.

[6] Malliaras, G. G.; Salem, J. R.; Brock, P. J.; Scott, C. Electrical characteristics and efficiency of single-layer organic light-emitting diodes. *Phys. Rev. B*, **1998**, *58*, 13411.

[7] Chu, T.-Y.; Song, O.-K. Hole Mobility of N,N '-bis(naphthalen-1-Yl)-N,N '-bis(phenyl) benzidine investigated by using space-charge-limited currents. *Appl. Phys. Lett.,* **2007**, *90*, DOI: 10.1063/1.2741055.